Journal of Nano- and Electronic Physics
Vol. **17** No 5, 05021(7pp) (2025)

Журнал нано- та електронної фізики
Том **17** № 5, 05021(7cc) (2025)

OPEN ACCESS

REGULAR ARTICLE

Spin Exchange *d-f* Interaction in Impedance Spectrum

K.A. Korotkov[1,*], V.V. Netyaga[1], Yu.O. Shkurdoda[2], A.I. Dmitriev[1]

[1] *Institute for Problems of Materials Science, National Academy of Sciences of Ukraine, Kyiv-142, Ukraine*
[2] *Sumy State University, 40007 Sumy, Ukraine*

(Received 23 July 2025; revised manuscript received 24 October 2025; published online 30 October 2025)

The experimentally observed decrease in the values of the reflection $R(f)$ for Fe/Gd_2O_3 nanostructures is due to the influence of the *d-f* exchange interaction. These changes make Fe/Gd_2O_3 nanostructures suitable for use in modulation polarimetry, resonator systems, and stealth technologies. The impedance spectroscopy of Fe nanofilms grown on Gd_2O_3 and silica glass (SiO_2) substrates in the frequency range of 0-10^7 Hz has been investigated. As the thickness of Fe nanofilms increases, their morphology changes from nanodot to labyrinth to percolation, consisting of iron islands that provide the percolation mechanism of conductivity. The complex morphology of foils is the source of the and capacitive components of the imaginary part of the impedance. The hodographs and corresponding equivalent circuits of nanofilms are analyzed. The comparison for Fe/SiO_2 and for Fe/Gd_2O_3 shows the closeness of their basic characteristics of dependence on h. The differences lie in the numerical values of the parameters. The latter are a function of the kinetic properties of the films and the influence of the *d-f* exchange interaction. In the frequency range $f > 10^5$ Hz, the $\varepsilon(f)$ dependences show a peculiarity in the form of a maximum. The formation of this peak is probably related to the spin noise effect. The spin noise effect is characteristic for films with tunneling conductivity.

Keywords: Impedance spectroscopy, Oxide nanofilms, Fe, Gd_2O_3, *d-f* exchange interaction.

DOI: 10.21272/jnep.17(5).05021 PACS number: 73.20. – r

1. INTRODUCTION

Exchange interaction increases the magnetization of ferromagnetic layers (Fe, Co, Ni, Fe_3O_4) [1, 2], thereby enhancing many properties of structures based on them, such as magneto-optical [3], electron paramagnetic resonance [4], galvanomagnetic [5], anomalous Hall effect [6], and conductivity of MDM structures [7]. Such amplification does not require energy or the use of amplifying devices and can be achieved at the nanoscale, which is important for nanotechnology.

The special radio-optical properties of Fe nanofilms (FeNF) are suggested by their porous morphology.

Modern methods of protection of aircraft from detection are united in stealth technology, a set of methods to reduce the probability of detection of objects in the radar field. In this case, the main task is to suppress reflectivity. Solving this problem by changing the geometry and configuration of flying objects has led to a significant reduction in their aerodynamic characteristics. Currently, the idea of coating reflective surfaces with absorbing (paints and varnishes with special fillers) or scattering microporous materials (specially treated fabrics, etc.) is used. The nanoporous morphology of FeNF may be of interest for stealth technology.

The aim of this work is to study the effect of the *d-f* exchange interaction on the radioptical properties of Fe/Gd_2O_3 nanostructures in the decimeter range. The decimeter range of combined arms radar radiation is used by military systems all armies of the world.

To achieve this goal, impedance spectroscopy in the frequency range 0-10^7 Hz of FeNF grown on Gd_2O_3 and silicate glass (SiO_2) substrates has been studied. In the latter case, the influence of the *d-f* exchange interaction is elucidated.

In FeNF, each pair of charged adjacent islands separated by a gap represents a capacitor with charge leakage due to electron conduction through the potential gap barrier. Within this framework, the study of the frequency dependence of the dielectric constant for Fe/SiO_2 and Fe/Gd_2O_3 nanostructures allows us to calculate their radio-optical properties.

2. CONDITIONS OF THE EXPERIMENT

The Fe and Gd_2O_3 films were deposited on a SiO_2 substrate by electron beam evaporation of targets of similar composition from chemically pure reagents. Deposition conditions were as follows: Fe – vacuum $p = 3 \cdot 10^{-3}$ Pa, film growth rate v = (5-10) nm/min, substrate temperature

* Correspondence e-mail: k.korotkov@ipms.kyiv.ua

© 2025 The Author(s). Journal of Nano- and Electronic Physics published by Sumy State University. This article is distributed under the terms and conditions of the Creative Commons Attribution (CC BY) license.

Cite this article as: K.A. Korotkov et al., *J. Nano- Electron. Phys.* 17 No 5, 05021 (2025) https://doi.org/10.21272/jnep.17(5).05021

t = (30-40) °C; Gd_2O_3 – chamber O_2 partial pressure $p_{O_2} = 2 \cdot 10^{-2}$ Pa, film growth rate v = (3-10) nm/min, substrate temperature t = (30-50) °C. For comparison, FeNF were deposited both on the Gd_2O_3 layer and directly on the silica glass (SiO_2) substrate. This allows us to determine the role of *d-f* exchange interaction in the parameters under study. The thickness of the Gd_2O_3 layer in all samples was 50 nm, and the thickness of the Fe layer varied within h = (5-70) nm. Cu film electrodes were applied to the ends of the FeNF by thermal evaporation to solder conductive wires.

To stabilize the resistance of FeNF, which increases due to oxidation in air after removal from the sputtering chamber, the samples were kept in the atmosphere at room temperature for 3 days. At the same time, the film was covered with a thin layer of oxide, which significantly slows down further oxidation and resistance changes, which made it possible to measure the impedance and its frequency dependence. The surface oxidation of the FeNF was not dangerous, since earlier in [5] we showed that the *d-f* exchange interaction occurs not only at the interface of the REM (rare earth metal) oxides with Fe, but also with Fe_3O_4. The Fe_3O_4 magnetite is a semi-metal in terms of conductivity, so it does not interfere with the passage of electrons through the FeNF with a complex morphology.

The following equipment was used for the experiments. The films were deposited on a VU-1A electron beam evaporation apparatus. Microscopic studies of the morphology of the films were performed on a Tescan Mira 3 LMU scanning electron microscope. Electrophase analysis of the FeNF was performed on a JEM 2100 F transmission electron microscope. The impedance frequency response was measured on a Solarton 1250 FRA using the ZPlot computer program. The data were analyzed using the ZView program.

3. MORPHOLOGY OF FE NANOFILMS

Fig. 1 shows the electron microscope images and electron micrographs of FeNF grown on a Gd_2O_3 layer. FeNF grown on silicate glass under similar conditions have similar morphology and structure.

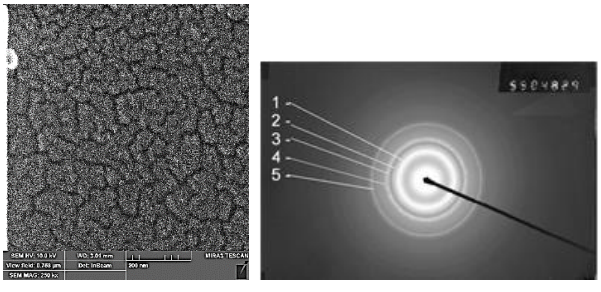

a b

Fig. 1 – The morphology of Fe (30 nm) nanofilms grown on Gd_2O_3 (50 nm) (a) and their electron pattern: 1-st line – Fe_3O_4 (d_1 = 0.2967 nm), 2-nd line – Fe_3O_4 (d_2 = 0.2532 nm), 3-rd line – Fe (d_1 = 0.20268 nm), 4-th line common for Fe (d_2 = 0.14332 nm) and Fe_3O_4 (d_3 = 0.1485 nm), 5-th line – Fe (d_3 = 0.11702 nm)

The morphology of FeNF grown on Gd_2O_3 is island-like. The film is formed by two structural types of iron islands, which differ in the size of the dielectric barrier between the iron particles. One structure is formed into large islands of clusters of iron particles of stochastic shape with size from 20 to 200 nm, separated by a dielectric barrier of 5-20 nm width and more than 200 nm length of labyrinth type. The second structure of iron islets appears as dense clusters of iron nanoparticles of stochastic shape, which actually form large islet structures. In clusters, nanoparticles are separated by an insignificant barrier, the size of which ranges from 1 to 10 nm. In such clusters, tunneling of electrons through a small dielectric barrier is possible. Thus, the object of research are island films with a system of numerous clusters of ferromagnetic nanoparticles separated by a small dielectric barrier-Taking into account the stability of technological modes of sputtering, it can be assumed that the morphologies of films for different thicknesses will differ mainly in the size of interstrand distances.

Electron phase analysis shows the presence of diffraction lines on electronograms corresponding to both pure iron and its oxide Fe_3O_4. [8]. The most probable model of Fe nano-island films after their oxidation in air is the core-shell configuration, where the core consists of Fe and the shell consists of Fe_3O_4 oxide, as shown in Fig. 2. At the distance between nanoparticles $l = 0$, the percalation mechanism of current transfer is realized, and at $l > 0$, the tunneling mechanism is realized [8].

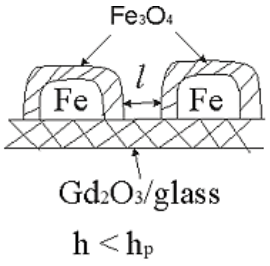

Fig. 2 – Schematic of the structure of Fe nano-island films after their oxidation in air, where h is the film thickness, h_p 30 nm. Film thickness at which the percalation threshold is reached.

4. RESULTS AND DISCUSSION

4.1 Nyquist Hodographs and Equivalent Substitution Schemes

To study the dielectric properties of the samples presented, we used the method of impedance spectroscopy [9], which consists in analyzing the impedance $Z(\omega = 2\pi f)$ and its components as a function of the AC frequency. A visual representation of the frequency behavior of the impedance $Z(\omega)$ can be obtained by constructing a hodograph (Nyquist diagram), which shows the trajectory of the change in the complex plane of the $Z(\omega)$ vector. The measurement results can be presented in the form of frequency dependencies of complex quantities: impedance $Z = Z' + jZ''$; admittance $Y = Y' + jY''$ ($Y = 1/Z$); dielectric constant

$\varepsilon = \frac{Y}{j\omega C_0} = \varepsilon' - j\varepsilon''$, where ε' and ε'' are the real and imaginary parts of the dielectric constant ε; C_0 is the capacitance of a capacitor with the same geometric dimensions as the one being measured, but filled with air.

The use of a hodograph is the basic and most visual way to represent the electrical properties of the measured samples by constructing equivalent circuits. An equivalent circuit is an electrical circuit consisting of ideal resistors, capacitors, and inductors that have the same frequency response as the measured sample. The numerical values of the impedances of the equivalent substitution schemes were calculated using the least squares method. Fig. 3 shows the equivalent substitution scheme for before and after the percolation threshold of Fe/SiO_2 and Fe/Gd_2O_3 nanostructures.

The Nyquist plots for prepercolation thicknesses of the FeNF of on SiO_2 (Fig. 4a) looks like semicircles intersecting the Z' axis at two points. As h increases, the area of the semicircle decreases. At $h > hp$ the hodograph changes sign and degenerates into a curved line (Fig. 4b) continuing to decrease in size for Fe/SiO_2. But not in the case

a b

Fig. 3 – Equivalent substitution scheme for pre-percolation (a) and post-percolation threshold (b) Fe/SiO_2 and Fe/Gd_2O_3 nanostructures

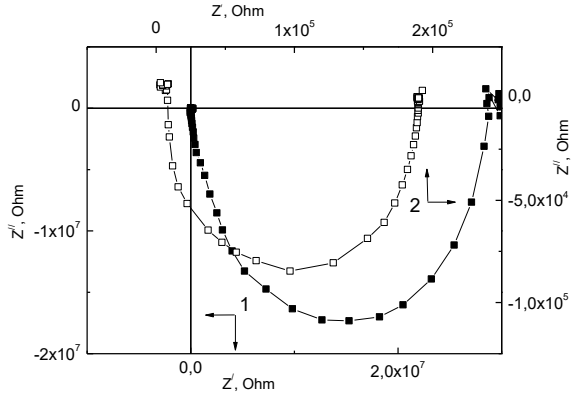

a

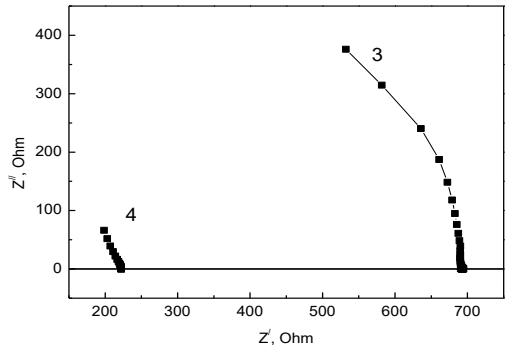

b

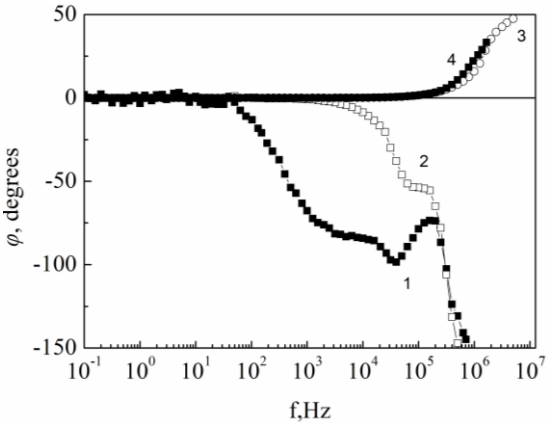

c

Fig. 4 – a, b: Nyquist hodographs of the Fe/SiO_2 nanostructures for FeNF with thicknesses of 13 nm (a, curve 1), 24 nm (a, curve 2), 35 nm (b, curve 3), and 66 nm (b, curve 4). 4 c. Frequency dependences of the phase angle φ(ω) between current and voltage

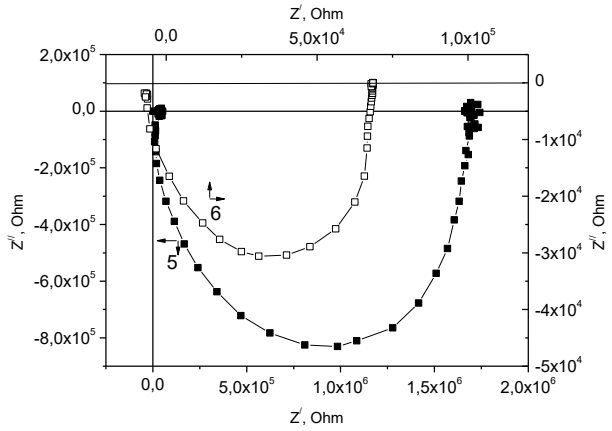

a

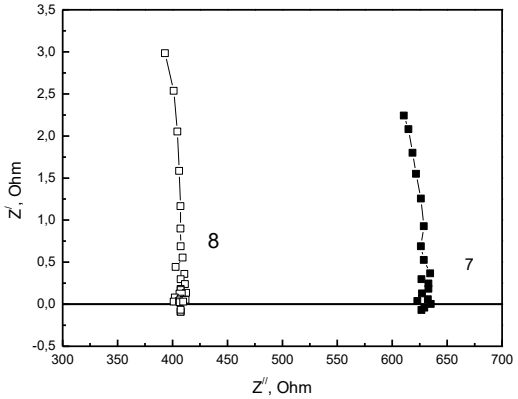

b

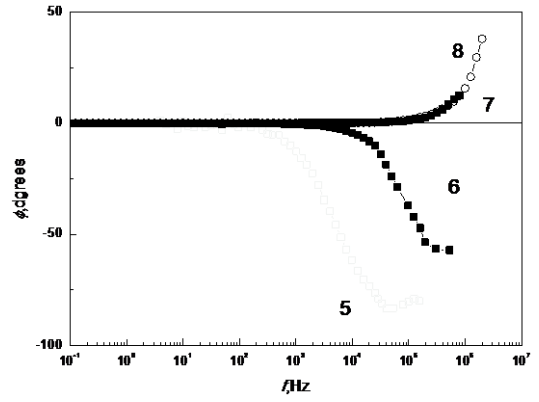

c

Fig. 5 – a, b: Nyquist hodographs of the Fe/Gd_2O_3 nanostructures for *FeNF* with thicknesses of 5 nm (a, curve 5), 11 nm (a, curve 6), 32 nm (b, curve 7), and 58 nm (b, curve 8). 5 c. Frequency dependences of the phase angle φ(ω) between current and voltage

Fe/Gd_2O_3 where the *d-f* exchange interaction leads to an increase in the magnetic moment of the nanostructure. This leads to the emergence of magnetoresistance and an increase in the size of the hodograph. This indicates a strong dependence nanostructures on its thickness of FeNF and *d-f* exchange interaction.

At high frequencies (leftmost point), $Z' \approx R1$ corresponds to the resistance of the conductive of the FeNF. At low frequencies (the right intersection of the hodograph with the Z' axis), the impedance value corresponds to the sum of the resistances of the Fe_3O_4 dielectric layer $R2$ and accounts for the resistance of the SiO_2 dielectric substrate (Fig. 3a), and the volume of the FeNF: $Z' = R1 + R2$. In Fig. 4c, 5c (curves 3, 4, 7, 8), the phase shift for these samples at frequencies $f \geq 10^3$ Hz indicates the capacitive nature of the impedance, i.e. the presence of a capacitance.

Thus, the resistive-capacitive coupling represented by parallel *RC* chains in the equivalent circuits indicates the island structure of the FeNF Since these films do not form an infinite cluster, the equivalent circuits contain two resistors in series (Fig. 3a). The second resistor R2 accounts for the resistance of the SiO_2 dielectric substrate. Resistor $R2$ is shunted by capacitor $C1$, whose capacitance is equal to the capacitance of the dielectric layer between the islands.

Comparison of Fig. 4 for Fe/SiO_2 and Fig. 5 for Fe/Gd_2O_3 nanostructures shows the similarity of their main characteristics. However, according to the comparison of almost identical Fe thicknesses, the Nyquist hodographs differ by several orders of magnitude (Fig. 6).

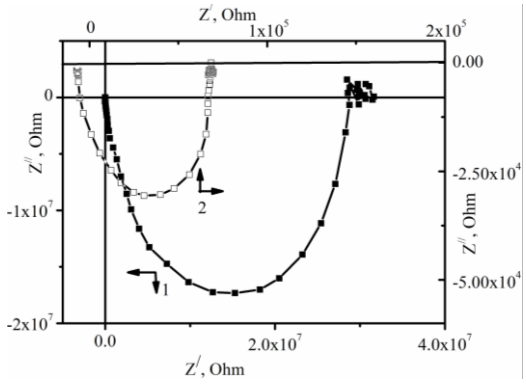

Fig. 6 – Nyquist hodographs of the nanostructures for samples with thicknesses of Fe/SiO_2 13 nm (curve 1), Fe/Gd_2O_3 (curve 2), 11 nm

The parameters of the equivalent circuit (Fig. 3) are calculated according to Fig. 4, 5 (Table 1).

Table 1 – Equivalent circuit parameters (Fig. 3) for Fe/SiO_2 and Fe/Gd_2O_3

Fe/SiO_2			Fe/Gd_2O_3		
13 nm			5 nm		
$R1$ (Ohm)	$C1$ (F)	$R2$ (Ohm)	$R1$ (Ohm)	$C1$ (F)	$R2$ (Ohm)
$1.1 \cdot 10^4$	$1.47 \cdot 10^{-11}$	$3.24 \cdot 10^7$	$9.24 \cdot 10^3$	$2.12 \cdot 10^{-11}$	$1.73 \cdot 10^6$
24 nm			11 nm		
$1.55 \cdot 10^4$	$1.81 \cdot 10^{-11}$	$1.75 \cdot 10^5$	$1.13 \cdot 10^4$	$2.72 \cdot 10^{-11}$	$5.72 \cdot 10^4$
35 nm			32 nm		
$R1$ (Ohm)	$L1$ (H)	$C1$ (F)	$R1$ (Ohm)	$L1$ (H)	$C1$ (F)
$6.92 \cdot 10^2$	$5.49 \cdot 10^{-5}$	$5.86 \cdot 10^{-11}$	$6.20 \cdot 10^2$	$5.08 \cdot 10^{-5}$	$5.86 \cdot 10^{-11}$
66 nm			58 nm		
$2.22 \cdot 10^2$	$5.49 \cdot 10^{-5}$	$3.34 \cdot 10^{-10}$	$4.07 \cdot 10^2$	$4.27 \cdot 10^{-5}$	$1.69 \cdot 10^{-10}$

Analysis of Table 1 shows that for the Fe/SiO_2 nanostructures at $h < 30$ nm, the conductivity is determined by electron tunneling between Fe nanoparticles forming a capacitor with a dielectric layer consisting of two Fe_3O_4 plates separated by an air gap of thickness l (see Fig. 2). Capacitance $C1$ increases slightly with increasing h (23.1 %) since $C \sim 1/l$ and at $l > 2$ nm. $C1 \cong$ const. The latter indicates that up to the percolation threshold, the distance between Fe nanoparticles $l > 2$ nm.

Resistance $R1$ is determined by the leakage currents of capacitance $C1$ and is symbatically related to it. The resistance value of the glass substrate $R2$ is determined by the hopping mechanism of conductivity. Since the effective hop length for conductivity is comparable to l, then $R2 \sim l$ and decreases by 2 orders of magnitude with increasing h,

$R2 >> R1$. At $h > 30$ nm, the percolation mechanism determines the conductivity. Therefore, the resistor $R3$ corresponds to the resistance of the conductive cluster, and $L1$ to its inductance, Fig. 3 (b). The value of $R3$ decreases with increasing h due to the increase in the number of infinite conductive clusters. The decrease in the value of $L1$ in this case can be explained by the example of the dependence of the inductance of a single-layer cylindrical coil without a core.

$$L\ [\mu H] \sim 1/I\ [cm] \tag{1}$$

where I is the length of the coil winding.

Let us assume that I is symbatical with the cluster length d increasing with h. Then, at 200 nm $\geq d \ll I = 1$ cm, the function (1) acquires the character of a strong dependence, which explains the changes in the value of $L1$. However, the value of $\varphi(\omega)$ does not exceed ≈40° and decreases to ≈ 20° (Fig. 4.5), which indicates a decrease in the role of inductance in the current transfer process with increasing h.

The increase in the capacitance of the capacitor $C2$ is associated with the tendency of $l \rightarrow 0$ in an increasing number of infinite clusters. Comparison for Fe/SiO_2 and for Fe/Gd_2O_3 shows the closeness of their main characteristics of deposition from h. The differences lie in the numerical values of the parameters under discussion. Which is confirmed by the example of their comparison with approximately equal thicknesses of FeNF (Fig. 6). The latter are a function of the kinetic features of the substrates.

4.2 Radio-Optical Parameters in the Decimeter Range

Porous materials are capable of absorbing and scattering radiation. Therefore, the nanoporous morphology of FeNF may be of interest for stealth technology. The experimental results of the impedance study for Fe/SiO_2 and Fe/Gd_2O_3 nanostructures make it possible to evaluate their radio-optical characteristics in the decimeter wave range.

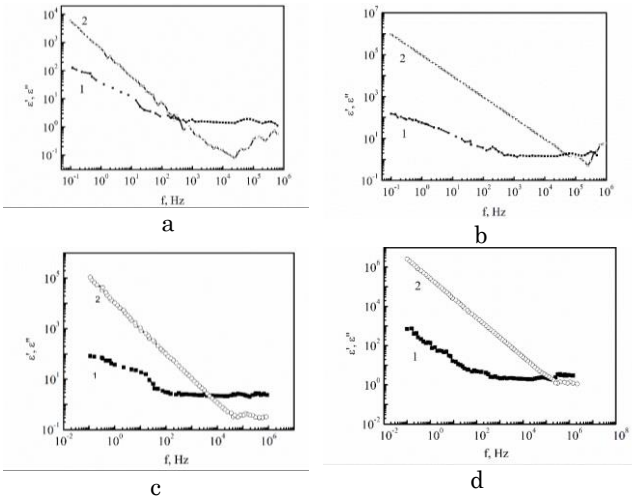

Fig. 7 – Frequency dependence of the dielectric constant ε in films with thicknesses of 13 nm (Fe/SiO_2) (a), 24 nm (Fe/SiO_2) (b), 5 nm (Fe/Gd_2O_3) (c) and 11 nm (Fe/Gd_2O_3) (d): $1 - \varepsilon'$, $2 - \varepsilon'$

Fig. 7 shows the frequency dependence of the dielectric constant for pre-percolation film thicknesses in Fe/SiO_2 and Fe/Gd_2O_3 nanostructures.

Based on the results of the experimentally measured impedances, Fig. 7 shows the calculated frequency dependences of the ε' real and ε'' imaginary components of the dielectric constant of nanostructures according to (2, 3) [10]:

$$\varepsilon' = \frac{Y''(\omega)}{(\omega)\varepsilon_0} = \frac{-Z''}{\left(Z'^2 + Z''^2\right)\omega\varepsilon_0}; \tag{2}$$

$$\varepsilon'' = \frac{Y'}{(\omega)\varepsilon_0} = \frac{Z'}{\left(Z'^2 + Z''^2\right)\omega\varepsilon_0}, \tag{3}$$

where ε_0 is the dielectric constant of the vacuum.

The large values of ε' and ε'' in the low frequency range (0.1 ÷ 100 Hz) are not real nanostructures parameters, but some effective values resulting from the uneven distribution of electric charges and field in the film and the presence of free charge conductivity. The linear dependence of ε'' in the frequency range of $0.1 \div 3 \cdot 10^4$ Hz is determined by the frequency dependence of the permeability $\sigma'(\omega)$ [11]:

$$\varepsilon'' = \frac{\sigma'(\omega)}{\omega\varepsilon_0} \tag{4}$$

As the frequency $f \geq 10^5$ Hz is increased, the phase shift (Fig. 4c, 5c) reaches values close to 90°, which corresponds to the capacitive bias current that is the main contributor to the polarization of the film islands. At the same time, there is no charge accumulation, resulting in a constant value of ε. For the sample 13 nm $\varepsilon \approx 1.4$, for the sample 24 nm $\varepsilon \approx 1.58$. From the calculated values of the real ε' (2) and imaginary ε'' (3) parts of the total dielectric constant ε can be calculated as follows

$$\varepsilon = \sqrt{\varepsilon'^2 + \varepsilon''^2} \tag{5}$$

Fig. 8 shows a typical frequency dependence of the dielectric constant for Fe/SiO_2 and Fe/Gd_2O_3 nanostructures.

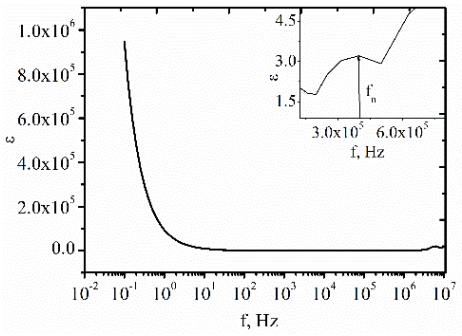

Fig. 8 – Typical frequency dependence of the dielectric constant $\varepsilon(f)$ for Fe/SiO_2 and Fe/Gd_2O_3 nanostructures. The insets show the dielectric constant in the range of $1 \div 8 \cdot 10^5$ Hz, f_n – frequency of spin noise extremes

According to the classical optical theory, the absorption coefficient $\alpha = \varepsilon - 1$ and the transmittance $T = 10^{-\alpha}$ can be calculated. From the absorption and transmittance coefficients, the reflection coefficient can be calculated.

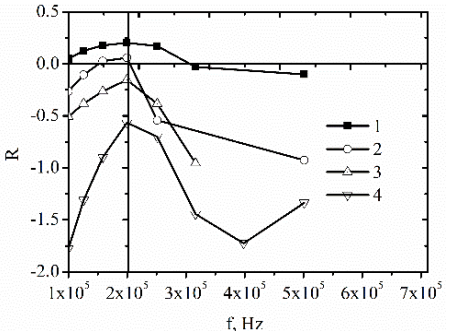

Fig. 9 – Frequency dependence of reflection coefficient $R(f)$ for Fe/SiO_2 nanostructures with Fe thicknesses of 13 nm (curve 1), 24 nm (curve 2), and Fe/Gd_2O_3 with Fe thicknesses of 5 nm (curve 3) and 11 nm (curve 4)

The experimentally observed decrease in the values of the reflection $R(f)$ for Fe/Gd_2O_3 nanostructures compared to the Fe/SiO_2 structure is due to the influence of the *d-f* exchange interaction of the ferromagnetic /oxide REM type [9].

The calculated para-optical (*para* is Latin for similarity) values of the reflection $R(f)$ for Fe/Gd_2O_3 nanostructures indicate the prospects of using such a structure in stealth technology [12].

In the frequency range $f > 10^5$ Hz, the dependences $\varepsilon(f)$ show a peculiarity in the form of a maximum (see Table 2).

Table 2 – The spin-noise extremes f_n for Fe/SiO_2 and Fe/Gd_2O_3 nanostructure

Fe/SiO_2			Fe/Gd_2O_3		
h_{Fe} (nm)	f_n (Hz)	ε	h_{Fe} (nm)	f_n (Hz)	ε
13	$4.023 \cdot 10^5$	2.15	5	$4.006 \cdot 10^5$	3.42
24	$3.936 \cdot 10^5$	3.17	11	$3.975 \cdot 10^5$	3.70
35	Not extremum		32	Not extremum	
66	Not extremum		58	Not extremum	

The formation of the peak is probably due to the spin noise effect [13]. The calculated values of $\varepsilon(f)$ are a consequence of experimental measurements of the electrical impedance parameters (2, 3, 5). For $h < h_p$, the current transfer mechanism is tunneling, determined by the spin-exchange *d-f* interaction [5, 7]. Therefore, the spin noise effect is characteristic of films with $h < h_p$. At $h > h_p$, the percalation mechanism of charge transfer is realized, where the influence of the spin interaction is not significant [5, 7]. This results in the absence of maxima for the $\varepsilon(f)$ dependence.

5. CONCLUSIONS

Impedance spectroscopy of Fe nanofilms grown on Gd_2O_3 and silicate glass (SiO_2) substrates in the frequency range of $0\text{-}10^7$ Hz has been studied. It is shown that with increasing thickness of Fe nanofilms, their morphology changes from nanodot to labyrinthine to continuous, consisting of coalesced iron islands that provide a percolation mechanism of conductivity. The most probable model of Fe nanofilms after their oxidation in air is the core-shell configuration, where the core consists of Fe and the shell is made of Fe_3O_4 oxide. Such a complex morphology of the nanofilms is the source of the induction and capacitive components of the imaginary part of the impedance. The analysis of Nyquist hodographs and corresponding equivalent circuits of nanofilms is carried out. Such a complex morphology of the films is the source of the induction and capacitive components of the imaginary part of the impedance. The Nyquist hodographs and corresponding equivalent circuits of the nanofilms are analyzed. The comparison for Fe/SiO_2 and Fe/Gd_2O_3 shows the closeness of their main characteristics of dependence on h. The differences lie in the numerical values of the parameters. The latter are a function of the kinetic properties of the films and the influence of the *d-f* exchange interaction.

In the frequency range $f > 10^5$ Hz, the dependences of $\varepsilon(f)$ show a peculiarity in the form of a maximum at frequency f_n. The formation of this peak is probably related to the spin noise effect. The spin noise effect is characteristic of films with $h < h_p$.

The experimentally observed increase in the values of the reflection coefficients $R(f)$ for Fe/Gd_2O_3 nanostructures compared to the Fe/SiO_2 structure is due to the influence of the *d-f* exchange interaction.

These changes make Fe/Gd_2O_3 nanostructures suitable for use in modulation polarimetry, resonator systems, and stealth technologies.

ACKNOWLEDGEMENTS

The authors are grateful to Grand PhD Doctor of Science B.K. Serdega, Grand PhD Doctor of Science O.Yu. Khizhun, PhD A.I. Ievtushenko for discussion, comments and recommendations, PhD A.M. Kasumov for discussion and preparation of unique samples.

The work was carried out at the expense of the budgetary topic of the National Academy of Sciences of Ukraine "Optical, magnetic and thermoelectric properties of the newest nanocomposites based on oxide materials" (code III-6-22).

REFERENCES

1. K. Kawaguchi, M. Sohma, T. Manago, *J. Magn. Magn. Mater.* **198-199**, 513 (1999).
2. J.M. De Teresa, A. Fernández-Pacheco, L. Morellon, et al, *J. Microelectron. Eng.* **84** No 5-8, 1660 (2007).
3. A.M. Kasumov, V.M. Karavayeva, K.O. Shapoval, et al., *Nanosistemi, Nanomateriali, Nanotehnologii* **16** No 1, 181 (2018).
4. H. Han, L. Zhang, H. Liu, et al., *Philos. Mag.* **95** No 27, 3014 (2015).
5. A.M. Kasumov, A.I. Dmitriev, M.V. Radchenko, et al., *Chem., Phys. Technol. Surf.* **13** No 1, 105 (2022).
6. S.N. Nikolaev, K.Y. Chernoglazov, V.A. Demin, et al., *J. Surf. Investig.* **11**, 549 (2017).
7. A.M. Kasumov, K.O. Shapoval, V.M. Karavayeva, et al., *Powder Metall. Met. Ceram.* **58**, 576 (2020).
8. A.M. Kasumov, A.I. Dmitriev, V.V. Netyaga, et al., *J. Nano-Electron. Phys.* **16** No 4, 04001 (2024).
9. H. Kumar, K.C. Kharkwal, K. Kumar, et al., *Phys. Rev. B* **101**, 064405 (2020).
10. K. Kumari, A. Vij, M. Hashim, et al., *AIP Conf. Proc.* **2006**, 030026 (2018).
11. S.K. Sharma, P. Thakur, Sh. Kumar, et al., *Thin Solid Films* **519** No 1, 410 (2010)
12. K.A. Korotkov, V.V. Netyaga, *APHYS-2024* (Kyiv: 25-27 October 2024).
13. Va S. Zapasskii, *Adv. Opt. Photon.* **5**, 131 (2013).

Спіновий обмін *d-f* взаємодії в імпедансному спектрі

К.А. Коротков[1], В.В. Нетяга[1], Ю.О. Шкурдода[2], А.І. Дмитрієв[1]

[1] *Інститут проблем матеріалознавства НАН України, Київ-142, Україна*
[2] *Сумський державний університет, 40007 Суми, Україна*

Експериментально спостережене зменшення значень відбиття $R(f)$ для наноструктур Fe/Gd_2O_3 зумовлене впливом *d-f* обмінної взаємодії. Ці зміни роблять наноструктури Fe/Gd_2O_3 придатними для використання в модуляційній поляриметрії, резонаторних системах і стелс-технологіях. Досліджено імпедансну спектроскопію наноплівок Fe, вирощених на підкладках Gd_2O_3 та кремнеземного скла (SiO_2) в діапазоні частот 0-10^7 Гц. Зі збільшенням товщини Fe наноплівок їх морфологія змінюється від наноточок до лабіринту до перколяції, що складається з залізних острівців, які забезпечують перколяційний механізм провідності. Складна морфологія фольги є джерелом ємнісної та ємнісної складових уявної частини імпедансу. Проаналізовано годографи та відповідні еквівалентні схеми наноплівок. Порівняння для Fe/SiO_2 та для Fe/Gd_2O_3 показує близькість їхніх основних характеристик залежності від h. Відмінності полягають у числових значеннях параметрів. Останні є функцією кінетичних властивостей плівок і впливу *d-f* обмінної взаємодії. В діапазоні частот $f > 10^5$ Гц на залежностях $\varepsilon(f)$ спостерігається особливість у вигляді максимуму. Утворення цього піку, ймовірно, пов'язане з ефектом спінового шуму. Ефект спінового шуму характерний для плівок з тунельною провідністю.

Ключові слова: Імпедансна спектроскопія, Оксидні наноплівки, Fe, Gd_2O_3, *d-f* обмінна взаємодія.